Condensed Phenoxazine Dimer and Its Radical Cation

Takayuki Miyamae, Makoto Haraguchi, Yoshimitsu Tachi,

Shuichi Suzuki, Masatoshi Kozaki, and Keiji Okada

Miyamae, T., Haraguchi, M., Tachi, Y., Suzuki, S., Kozaki, M., & Okada, K. (2020). Condensed Phenoxazine Dimer and Its Radical Cation. *Organic Letters*, 22(17), 6790–6793. https://doi.org/10.1021/acs.orglett.0c02305

Condensed Phenoxazine Dimer and Its Radical Cation

Takayuki Miyamae,[†] Makoto Haraguchi,[†] Yoshimitsu Tachi,[†] Shuichi Suzuki,[§,*] Masatoshi Kozaki[†,‡,*] and Keiji Okada[†,‡,‖]

[†]Graduate School of Science, Osaka City University, Sugimoto, Sumiyoshi-ku, Osaka 558–8585 (Japan)

[‡]Osaka City University Advanced Research Institute for Natural Science and Technology (OCARINA) Sugimoto, Sumiyoshi-ku, Osaka 558-8585 (Japan)

[§]Graduate School of Engineering Science, Osaka University, Toyonaka, Osaka 560-8531 (Japan)

Supporting Information Placeholder

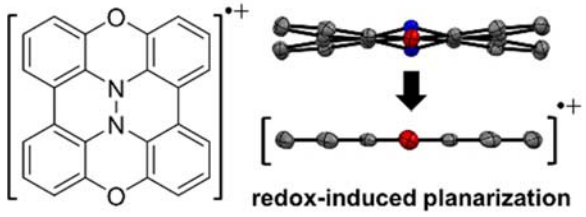

ABSTRACT: Condensed phenoxazine dimer was synthesized and characterized. X-ray crystallographic analysis of the dimer shows a double-butterfly structure, in which the nitrogen atoms are located above and below the molecular plane. Radical cation salt of the dimer was obtained using tris(4-bromophenyl)aminium hexafluoroantimonate as the oxidant. The salt is air-stable in solid and solution states. The cation structure was evaluated by X-ray crystallographic analysis, showing that the phenoxazine units were converted to a planar structure upon oxidation.

Radical cations of condensed polycyclic aromatic compounds are an important class of materials in the development of organic electronic, optical, and magnetic devices.[1] Phenothiazine **PTZ** and phenoxazine **PXZ** produce stable radical cations upon one-electron oxidation, converting the unique butterfly structure into planar.[2] The structural transformation is followed by a dramatic change in the photophysical properties and π-electron delocalization. Phenothiazine and phenoxazine skeletons are deemed to be attractive frameworks for materials with redox-responsive functions, owing to these desirable properties.[3] Incorporation of phenothiazine or phenoxazine skeletons in condensed polycyclic systems may produce compounds that exhibit excellent stimulus-responsive properties like **PTZ** and **PXZ**. The isolation and investigation of radical cations are essential to determine the differences in structural and electronic properties between neutral and oxidized states. However, only a few studies have reported on the isolation and structural elucidation of cationic species of condensed polycyclic compounds using phenothiazine or phenoxazine skeletons. In a recent work, we described the redox-induced planarization of polycyclic aromatic compounds using the phenoxazine substructure, trioxytriphenylamine **TOT**, and its application in the development of redox-responsive magnetic materials (Figure 1).[3c,d,4]

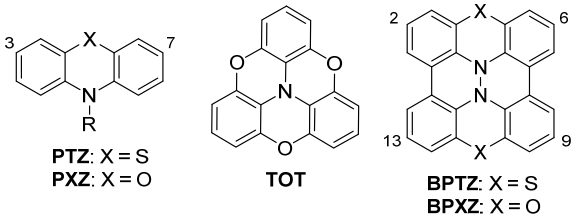

Figure 1. Chemical structure of electron donors with phenothiazine or phenoxazine substructures.

In the course of our attempts to explore condensed polycyclic aromatic systems with redox-induced planarization, we have focused on the condensed phenothiazine dimer **BPTZ**, previously reported by Higashibayashi et al.[5] **BPTZ** has a characteristic double butterfly structure, but the molecular structure of the radical cation has not been described yet. Theoretical studies using density functional theory (DFT) calculations were carried out, suggesting that **BPTZ**$^{\bullet+}$ has a non-planar structure, owing to the long C-S bond lengths. Shortening the carbon-heteroatom bond

length by replacing sulfur with oxygen atoms in **BPTZ** is a reasonable strategy to achieve non-planar to planar transformation upon oxidation. This approach is further supported by theorical studies. Herein, we synthesized the condensed the phenoxazine dimer **BPXZ** and successfully isolated its radical cation. The molecular structures of **BPXZ** and **BPXZ**$^{\bullet+}$ were investigated by X-ray crystallographic analysis.

Scheme 1. Synthesis of **BPXZ**.

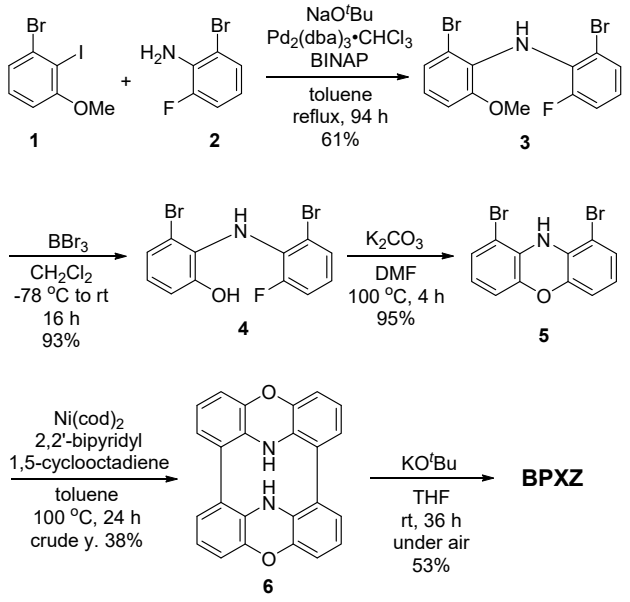

Scheme 1 illustrates the synthetic method to fabricate **BPXZ**. First, 3-bromo-2-iodoanisole (**1**) was synthesized according to a previously reported method.[6] Following this, diarylamine **3** was obtained by the Buchwald-Hartwig cross-coupling reaction of **1** and 2-bromo-6-iodoaniline (**2**).[7] Deprotection of the hydroxy group in **3** was carried out using BBr_3, followed by the intramolecular aromatic nucleophilic substitution in the presence of K_2CO_3, thereafter producing 1,9-dibromo-10*H*-phenoxazine (**5**).[4] The conversion of **5** into **BPXZ** was realized by slightly modifying the dimerization protocol developed by Higashibayashi as follows:[5] phenoxazine dimer **6** was fabricated by the nickel-mediated homo-coupling reaction of **5**. N-N bond formation was achieved by the aerobic oxidation of **5** under alkaline conditions, generating **BPXZ** as a red solid in 53% yield. Although **BPXZ** has a low solubility in common organic solvents, the structure of **BPXZ** was undoubtedly identified by MS, NMR, and X-ray structural and elemental analysis. **BPXZ** is stable under aerated conditions at room temperature in solid and solution states (Figure S1).

Single crystals of **BPXZ** suitable for X-ray crystallographic analysis were grown via the slow evaporation of THF from the solution. Four crystallographically independent molecules of **BPXZ** with almost identical structures in a unit cell were identified (Figure S3);[8] Figures 2a-c displays one of the identified **BPXZ** structures. As expected, **BPXZ** adopts a non-planar structure, where each phenoxazine unit has flat butterfly shape with a dihedral angle of 167°–169° between the two benzene rings, bent in the opposite direction. Two oxygen atoms are closer to the mean square plane formed by carbon atoms, and two nitrogen atoms are positions above and below the mean square plane. The deviations out of the plane were 0.25–0.29 Å and 0.36–0.37 Å for oxygen and nitrogen atoms, respectively (Figure 2b,c). The sum of C–N–C bond angles around each nitrogen atom is 336–337°, suggesting that the nitrogen atoms have significant sp^3 hybridization. The N–N bond lengths were 1.48–1.49 Å which are longer than those reported for tetraphenylhydrazine derivatives (1.38–1.43 Å).[5a] This can be attributed to the electronic repulsion between lone pair electrons of the nitrogen atoms. Moreover, N–N bond elongation was reported for **BPTZ** and its derivatives (1.44–1.50 Å).[5] **BPXZ** molecules are arranged in 1-D slip-stacked columns along the *b*-axis with close contacts between the carbon atoms (3.38 Å) and the carbon and oxygen atoms (3.21 Å) (Figure 3a). These distances are slightly shorter than the sum of the van der Waals radii (C-C: 3.40 Å and C-O: 3.22 Å).[9]

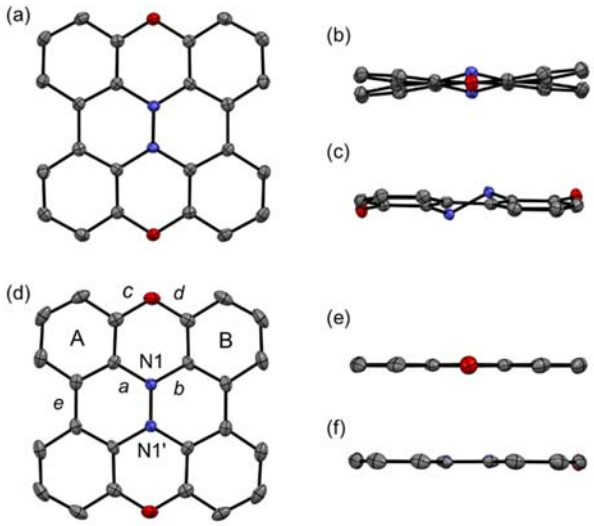

Figure 2. ORTEP views of **BPXZ** (upper) and **BPXZ**$^{\bullet+}$•SbF_6^- (lower) (50% probabilities): Top (a) and (d) and side views (b), (c), (e) and (f). Hydrogen atoms and counter anions were omitted for clarity. Grey, blue, and red ellipsoids represent carbon, nitrogen, and oxygen atoms, respectively.

Table 1. The selected bond lengths[a] and the bond and dihedral angles of **BPXZ** and **BPXZ**$^{\bullet+}$.

bonds and angles[b]	**BPXZ**[c]	**BPXZ**$^{\bullet+}$•SbF_6^-
N-N	1.49	1.37
a (C-N)	1.43	1.41
b (C-N)	1.43	1.40
c (C-O)	1.38	1.37
d (C-O)	1.38	1.37
e (C-C)	1.48	1.46
Sum of bond angles around the nitrogen atom	336-337°	360°
Dihedral angles between A and B rings	167-169°	180°

[a]In Å unit. [b]The assignment of bond names are shown in Figure 2. [c]Obtained from one of the independent molecules.

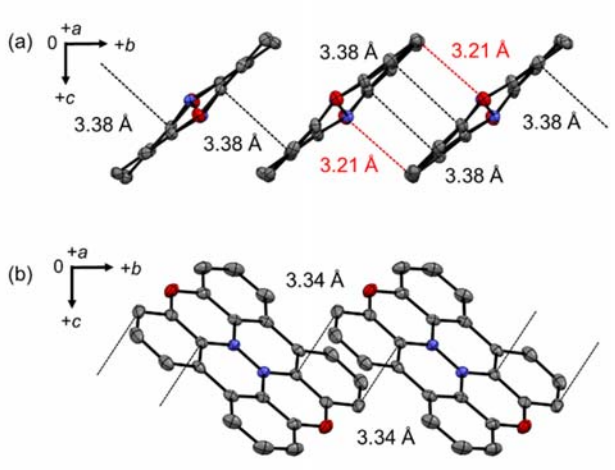

Figure 3. ORTEP views of crystal packing motifs of **BPXZ** (a) and **BPXZ**$^{\bullet+}$•SbF_6^- (b) (50% probabilities) Hydrogen atoms and counter anions were omitted for clarity. Grey, blue, and red ellipsoids represent carbon, nitrogen, and oxygen atoms, respectively. Dash lines show short C-C (black) and C-O contacts (red).

To evaluate the stability of the radical cation **BPXZ**$^{\bullet+}$, cyclic voltammograms of **BPXZ** were measured in degassed THF in the presence of 1.0 M tetra-*n*-butylammonium perchlorate as a supporting electrolyte (Figure 4). A reversible redox wave was observed at $E_{1/2}{}^{0/+1} = -0.20$ V vs Fc/Fc^+ because of the formation of **BPXZ**$^{\bullet+}$, indicating that **BPXZ**$^{\bullet+}$ is stable under these conditions. Neither the second oxidation nor the reduction wave was observed under the conditions of CV measurement. The first oxidation potential of **BPXZ** is slightly lower than that reported for **BPTZ** ($E_{1/2}{}^{0/+1} = -0.12$ V).[5b] The low oxidation potential alludes to the strong electron-donating ability of **BPXZ**.

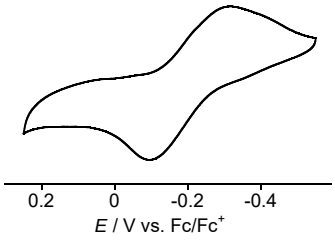

Figure 4. Cyclic voltammogram of **BPXZ** in THF in the presence of 0.1 M nBu_4NClO_4; V vs $Fc/Fc^+ = 0$ V (+0.55 V vs SCE), working electrode: glassy carbon, counter electrode: platinum, reference electrode: SCE, scan rate 100 mV/s.

Chemical oxidation of **BPXZ** was carried out in CH_2Cl_2 at room temperature using tris(4-bromophenyl)aminium hexafluoroantimonate as the oxidant. The desired radical cation salt **BPXZ**$^{\bullet+}$•SbF_6^- was obtained as a blue solid in 83% yield and its purification was achieved via the reprecipitation of the CH_3CN solution using diethyl ether. The structure and properties of **BPXZ**$^{\bullet+}$•SbF_6^- were characterized by MS, EPR (electron paramagnetic resonance), X-ray crystallography and elemental analysis. The UV–vis–near infrared (NIR) spectrum of **BPXZ**$^{\bullet+}$•SbF_6^- in CH_3CN (Figure 5) exhibited characteristic bands with absorption maxima at 633 and 693 nm. Time-dependent DFT calculations (UB3LYP/6-31G**//UB3LYP/6-31G**) suggested that the low-energy absorption band originates from the HOMO-1-HOMO (SOMO) transition ($f = 0.0658$) (Figure S2, Table S3). Moreover, **BPXZ**$^{\bullet+}$•SbF_6^- in CH_3CN exhibited negligible spectral change after 24 h under aerated conditions at room temperature (Figure S2), indicating the highly stable nature of **BPXZ**$^{\bullet+}$ under these conditions.

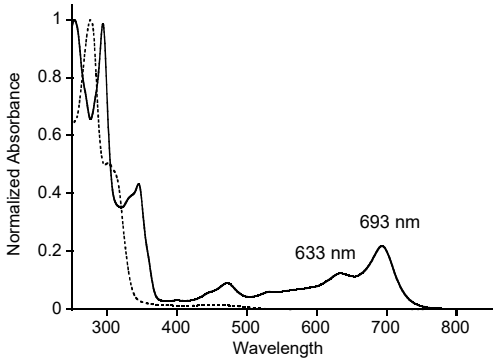

Figure 5. UV-vis-NIR absorption spectra of **BPXZ** in THF (dashed line) and **BPXZ**$^{\bullet+}$•SbF_6^- (solid line) in CH_3CN.

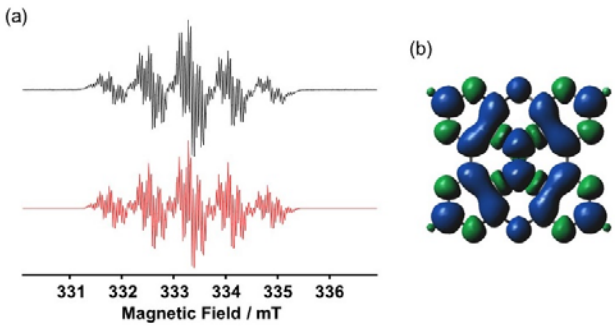

Figure 6. EPR spectra of **BPXZ**$^{\bullet+}$; observed in degassed CH_3CN at room temperature, 9.346338 GHz, $g = 2.0033$ (upper, black line) and simulated (lower, red line). Parameters for the simulation: $|a(^{14}N)| = 0.761$ mT, $|a(^{1}H)| = 0.175$ mT, 0.0489 mT, 0.0366 mT. (b) Spin density map of **BPXZ**$^{\bullet+}$ calculated at the DFT UB3LYP/6-31G** level (isovalue = 0.0004, blue positive spin, green: negative spin).

To gain further inside into the electronic structure, the EPR spectrum of **BPXZ**$^{\bullet+}$•SbF_6^- was obtained in degassed CH_3CN at room temperature. Multiple split lines with $g = 2.0033$ were observed (Figure 6). This spectral lines were successfully reproduced using spectral simulation with the following hyperfine coupling constants: ^{14}N nuclei ($I = 1$), $a(^{14}N) = 7.17 \times 10^{-4}$ cm^{-1} (0.761 mT); the three sets of ^{1}H nuclei ($I = 1/2$): $|a(^{1}H)|$ (×4) $= 1.65 \times 10^{-4}$ cm^{-1} (0.175 mT), $|a(^{1}H)|$ (×4) $= 4.61 \times 10^{-5}$ cm^{-1} (0.0489 mT), and $|a(^{1}H)|$ (×4) $= 3.45 \times 10^{-5}$ cm^{-1} (0.0366 mT). The largest coupling constant of ^{1}H nuclei was reasonably assigned, with the aid of the theoretical calculations, to the four equivalent ^{1}H nuclei at the 2, 6, 9, and 13-positions of **BPXZ** (Figure 6b), suggesting that the incorporation of a radical unit at these positions leads to a stronger spin-spin coupling. These results indicate that the electron spin of **BPXZ**$^{\bullet+}$ is delocalized over the

entire π-conjugated system. Low temperature EPR of **BPXZ**$^{\bullet+}$ in solid sample was measured at 110 K. Unfortunately, no notable intermolecular magnetic interaction is observed (Figure S6).

Single crystals of **BPXZ**$^{\bullet+}$•SbF_6^- suitable for X-ray crystallographic analysis were obtained via slow diffusion of ether into the benzonitrile solution of **BPXZ**$^{\bullet+}$•SbF_6^-. The observed molecular structure of **BPXZ**$^{\bullet+}$ is shown in Figure 2d-f. **BPXZ**$^{\bullet+}$ presents a planar structure with a dihedral angle of 180° between rings A and B, and an inversion center located in the middle of the N1-N1' bond. The summation of C-N-C bond angles around the nitrogen atom increased to 360° upon oxidation, indicating that the nitrogen atoms have an sp^2 hybridization instead of sp^3. The N1-N1' bond-length was significantly shortened from 1.49 Å to 1.37 Å upon oxidation because of the reduction in electron repulsion between the unshared electrons of the nitrogen atoms (Table 1). These results confirm that, upon oxidation, the BPXZ unit structure was converted from non-planar double butterfly to planar. In addition, the bond length analysis showed that all C-O, C-N, and C-C bonds bridging the two phenoxazine units are shorter than the corresponding bonds in neutral **BPXZ**, indicating π-electron delocalization over the entire molecule. HOMA (harmonic oscillator model of aromaticity) indexes were evaluated for heteroatom-containing rings in **BPXZ** (0.0405) and **BPXZ**$^{\bullet+}$ (0.270).[10] These HOMA indexes indicated that the aromatic character of the heteroatom-containing ring is enhanced upon oxidation. **BPXZ**$^{\bullet+}$ molecules formed 1-D slipped π-stacks along the *b*-axis with interplanar distances of 3.34 Å. This distance is shorter than the sum of van der Waals radii of carbon atoms (3.40 Å) (Figure 3b). The stacking columns were aligned along the *c*-axis with a short contact between the carbon and oxygen atoms (3.28 Å) (Figure S5).

In conclusion, a condensed phenoxazine dimer was synthesized and oxidized to produce its stable radical cation salt, which was isolated as a blue solid. Electrochemical measurements revealed that the condensed dimer is a strong electron donor. Crystal structures of the neutral species and radical cation salt were elucidated using X-ray crystallographic analysis. The neutral species adopts a characteristic double-butterfly structure, while the radical cation exhibited a planar structure. These results suggest that the condensed dimer is attractive for application as building blocks in redox-responsive magnetic materials.

ASSOCIATED CONTENT

Supporting Information

The Supporting Information is available free of charge on the ACS Publications website.
Detailed experimental procedures, characterization data, X-ray data with packing structure, copies of ^1H and ^{13}C NMR spectra of products, and DFT-calculations.

Accession Codes

CCDC 2014695 (**BPXZ**) and 2014696 (**BPXZ**$^{\bullet+}$•SbF_6^-) contains the supplementary crystallographic data for this paper. These data can be obtained free of charge via www.ccdc.cam.ac.uk/data_request/cif, or by emailing data_request@ccdc.cam.ac.uk, or by contacting The Cambridge Crystallographic Data Centre, 12 Union Road, Cambridge CB2 1EZ, UK; fax: +44 1223 336033.

AUTHOR INFORMATION

Corresponding Author

*E-mail: suzuki-s@chem.es.osaka-u.ac.jp
*E-mail: kozaki@sci.osaka-cu.ac.jp

Author Contributions

All authors have given approval to the final version of the manuscript.

Notes

[l]deceased

ACKNOWLEDGMENT

This work was partially supported by Grant-in-Aid for Scientific Research (JSPS KAKENHI #Grant Numbers, JP15H00956 (K.O.) JP17K05790 (M.K. and K.O.) and JP26102005 (S.S), JP17K05783 (S.S)).

REFERENCES

(1) (a) Organic Redox Systems (Ed.: T. Nishinaga), John Wiley & Sons, Inc., New Jersey, 2016. (b) Hirai, M.; Tanaka, N.; Sakai, M.; Yamaguchi, S. *Chem. Rev.* **2019**, *119*, 14, 8291–8331. (c) Sucunza, D.; Cuadro, A. M.; Alvarez-Builla, J.; Vaquero, J. J. *J. Org. Chem.* **2016**, *81*, 10126–10135. (d) Abe, M. *Chem. Rev.* **2013**, *113*, 7011–7088.

(2) (a) Oka, H. *Org. Lett.* **2010**, *12*, 448–451. (b) Tahara, T.; Suzuki, S.; Kozaki, M.; Shiomi, D.; Suigisaki, K.; Sato, K.; Takeji, T.; Miyake, Y.; Hosokoshi, Y.; Nojiri, H.; Okada, K. *Eur. J. Chem.* **2019**, 25, 7201–7209. (c) Suzuki, S.; Maya, R.; Uchida, Y.; Naota, T. *ACS Omega*, **2019**, *4*, 10031-10035.

(3) (a) Satoh, Y.; Catti, L.; Akita, M.; Yoshizawa, M. *J. Am. Chem. Soc.* **2019**, *141*, 12268–12273. (b) Suzuki, S.; Nagata, A.; Kuratsu, M; Kozaki, M.; Tanaka, R.; Shiomi, D.; Sugisaki, K.; Toyota, K.; Sato, K.; Takui, T.; Okada, K. *Angew. Chem. Int. Ed.* **2012**, *51*, 3193–3197. (c) Kuratsu, M.; Suzuki, S.; Kozaki, M.; Shiomi, D.; Sato, K.; Takui, T.; Kanzawa, T.; Hosokoshi, Y.; X.-Z. Lan, Y. Miyazaki, A. Inaba, K. Okada, K. *Chem. Asian J.* **2012**, *7*, 1604–1609.

(4) Kuratsu, M.; Kozaki, M.; Okada, K. *Angew. Chem. Int. Ed.* **2005**, *44*, 4056–4058.

(5) (a) Yamamoto, K.; Higashibayashi, S. *Chem. Eur. J.* **2016**, *22*, 663–671. (b) Shindo, Y.; Nomura, S.; Saikawa, Y.; Nakata, M.; Tanaka, K.; Hanaya, K.; Sugai, T.; Higashibayashi, S. *Asian J. Org. Chem.* **2018**, *7*, 1797–1801.

(6) (a) Sanz, R.; Castroviejo, M. P.; Fernandez, Y.; Fananas, F. J. *J. Org. Chem.* **2005**, *70*, 6548–6551. (b) Sanz, R.; Castroviejo, M. P.; Guilarte, V.; Perez, A.; Fananas, F. J. *J. Org. Chem.* **2007**, *72*, 5113–5118.

(7) Wolfe, J. P.; Wagaw, S.; Marcoux, J.-F.; Buchwald, S. L. *Acc. Chem. Res.* **1998**, *31*, 805–818.

(8) One of four molecules has disorder in its structure.

(9) Bondi, A. *J. Phys. Chem.* **1964**, *68*, 441–451.

(10) Krygowski, T. M.; Szatylowicz, H.; Stasyuk, O. A.; Dominikowska, J.; Palusiak, M. *Chem. Rev.* **2014**, *114*, 6383–6422.